![Aalto University logo](A! Aalto University)

Boisvert, G.; Lewis, L.J.; Puska, M.J.; Nieminen, R.M.

Energetics of diffusion on the (100) and (111) surfaces of Ag, Au, and Ir from first principles

Energetics of diffusion on the (100) and (111) surfaces of Ag, Au, and Ir from first principles

Ghyslain Boisvert* and Laurent J. Lewis†

Département de Physique et Groupe de Recherche en Physique et Technologie des Couches Minces, Université de Montréal, Case Postale 6128, Succursale Centre-Ville, Montréal, Québec, Canada H3C 3J7

Martti J. Puska and Risto M. Nieminen

Laboratory of Physics, Helsinki University of Technology, 02150 Espoo, Finland

First-principles calculations using the full-potential linear-muffin-tin-orbital technique have been performed to determine the energy barriers for adatom homodiffusion on the (100) and (111) surfaces of Ag, Au, and Ir. Our results agree very well with the measured energy barriers (when available), i.e., to within 0.03 eV, thereby confirming the adequacy of the theoretical method. On the (111) surfaces, we find that the barriers for Ag and Ir have values that are close to those corresponding to the melting point of the bulk materials, and conclude that "correlated jumps" should be present at high temperatures on these surfaces. For Au(111), on the other hand, the barrier is about twice as large as the melting temperature, and the random-walk model should provide an accurate description of the diffusion process, just as on the (100) surfaces, where the barriers are much larger. Semiempirical models are found to reproduce the first-principles energy barriers within 0.2 eV, which, in some cases, means errors as large as 90%.

I. INTRODUCTION

Diffusion is central to many physical processes which determine the topology and quality of surfaces — such as step flow, nucleation, and growth — and may involve the motion of adatoms, clusters, and step edges.[1-3] As a first step in characterizing mass transport on surfaces, the diffusion coefficient of single adatoms must be determined. Indeed, because diffusion usually follows an Arrhenius temperature dependence,[4] $D = D_0 \exp[-E_A/k_B T]$, the energy barrier E_A needs to be known with great accuracy in order to ensure a proper description of the phenomenon over a wide range of temperatures.

The diffusion coefficient is given in terms of the ensemble-averaged mean-square displacement $\langle R(t)^2 \rangle$ by the Einstein relation

$$D = \lim_{t \to \infty} \frac{\langle R(t)^2 \rangle}{2dt}, \qquad (1.1)$$

where d is the dimensionality of the space where diffusion is taking place ($d = 2$ for a flat surface). Because the mean-square displacement must be measured at several temperatures and for sufficiently long times, the experimental determination of energy barriers using such methods as field-ion microscopy (FIM), or more recently scanning-tunneling microscopy, is tedious and time consuming.[5] As a consequence, only very few systems have been studied up to now,[6-14] most of them containing $5d$ transition metals (in particular Ir and Pt), which are the most suitable for FIM studies.

From the theoretical point of view, diffusion coefficients can, in principle, be obtained from atomistic-simulation methods, such as Monte Carlo or molecular dynamics, given a proper model for the interatomic potentials. Empirical and semiempirical models have indeed been been used to calculate the mean-square displacements for diffusion on surfaces, yielding important and interesting insights into the phenomenon. Such models, however, are not always sufficiently accurate to provide a realistic picture of the materials studied, and *ab initio* (first-principles) techniques are sometimes called for. On the other hand, because of computer limitations, it is not yet feasible to study diffusion *per se*, while it is possible to calculate statically the energy barriers for diffusion.

We present, here, the results of a series of first-principles calculations of barriers for diffusion on the (100) and (111) surfaces of the transition metals Ag, Au, and Ir, using the full-potential linear-muffin-tin-orbital (FP-LMTO) method.[15] This follows from a previous study[16] of surface diffusion and diffusion barriers for Ag and Au using the semiempirical embedded-atom method (EAM),[17] in which we have demonstrated that the activation energy for adatom diffusion E_A is identical, within a few tens of meV, to the static energy barrier between two equilibrium sites; thus, the dynamical contributions of the substrate to the diffusion barriers are, in general, negligible. Moreover, we have shown recently that the prefactor D_0 is related to the energy barrier through a simple scaling relation, the compensation law, also known the Meyer-Neldel rule.[18] Thus, diffusion can be inferred from a knowledge of the static energy barriers, which can be accurately calculated using first-principles techniques.

We have also found in our EAM study[16] that diffu-

sion becomes non-Arrhenius at temperatures of the order of, or higher than, about half of the static energy barrier. This is due to the existence, at such "high" temperatures, of correlations between successive jumps, leading to mean-square displacements larger than those predicted by the random-walk model.[4] As a consequence, for surfaces where the energy barrier is small (smaller, say, than the melting temperature), it is necessary, in order to properly describe the diffusion process, to take such correlations into account at high temperatures. As a specific example, Jones et al.[9] reported diffusion data in the temperature range 500–800 K for Ag(111). Our EAM model predicts $E_A = 0.055$ eV for this surface, corresponding to about 640 K, obtained from fitting to the low-temperature data. (The Arrhenius law is valid, strictly speaking, only in the limit $T \to 0$.) However, we obtain $E_A = 0.1$ eV when fitting in the 500–800-K range, in qualitative agreement with the result of 0.15 eV by Jones et al. (although, as we will see below, the agreement is to some extent fortuitous.)

The purpose of the present study is threefold. First, it provides much-needed information on barrier heights for diffusion on metallic surfaces, as well as a consistent set of data against which experimental results can be compared. We examine here, following our previous EAM investigation,[16] the (100) and (111) surfaces of Ag and Au, as well as Ir, for which very good low-temperature experimental data are available.[8,10,13] Second, detailed knowledge (i.e., from first principles) of the height of the energy barriers, in particular relative to the melting temperature, will provide some indication of the validity of the random-walk model in describing surface diffusion. And third, our study will serve as a reference for assessing the validity of EAM for this problem.

In order to keep the problem as simple (and tractable) as possible, we consider all surfaces to be unreconstructed. Reconstruction, indeed, can have dramatic effects on diffusion. For instance, in the case of Au(111), which reconstructs into a $23 \times \sqrt{3}$ pattern,[19] we have shown, using EAM, that diffusion becomes strongly anisotropic,[20] proceeding preferentially along the "channels" arising from the presence of one extra atom every 23 along the x axis; a similar effect has been observed on the (110) surface of several fcc metals.[21] [Of the other surfaces studied here, Ir(100) (Ref. 22) and Au(100) (Ref. 23) also reconstruct.] Likewise, we limit ourselves to the case where diffusion proceeds by jumps although, in some cases, diffusion can also proceed via an exchange mechanism. This is well known for the (100) surfaces of fcc metals,[8,10–12,14,24] and has recently been found, on the basis of first-principles calculations, to be the favored mechanism for in-channel diffusion on Al(110).[25] During an exchange process, a surface atom is promoted above the surface, thus inducing large perturbations, which can only be dealt with using prohibitively large systems.

Our calculations are carried out within the framework of the density-functional theory,[26] known to give very accurate total-energy differences (within a small fraction of an eV for systems with comparable chemical properties). Since first-principles calculations are computationally intensive, it is common to deal with core electrons in the pseudopotential approximation and to expand the wave functions into plane waves. However, the systems under study here have very deep pseudopotentials, and therefore cannot be treated very efficiently using plane waves. Although the use of ultrasoft pseudopotentials can be envisaged, we chose, rather, to employ the all-electron FP-LMTO method,[15] with the wave functions developed into a small number of localized orbitals. The method has already been applied succesfully to the study of relaxation, reconstruction, and vacancy formation on noble and transition metal surfaces.[27–29]

Our results for the energy barriers agree very well with available experimental ones — to within 0.03 eV, confirming the accuracy of the method. On the (111) surfaces, we find that the barriers for Ag and Ir have values that are close to those corresponding to the melting points of the bulk materials. We conclude, therefore, that correlated jumps should be present at high temperatures on these surfaces. For Au(111), the barrier is about twice as large as the melting temperature, and the random-walk model should provide an accurate description of the diffusion process, just as on the (100) surfaces, where the barriers are much larger. Semiempirical models are found to reproduce the first-principles energy barriers within 0.2 eV which, in some cases, translates into errors as large as 90%.

Our paper is organized as follows. In Sec. II, we give details of the computational procedure used to calculate the energy barriers. In particular, we describe the supercell-slab model for the adatom at the equilibrium and transition states. This model requires, as input, the lattice constant for the bulk materials and the relaxation of the top layer. Results for these two properties are detailed in Secs. III A and III B. In Sec. III C, we present the results for the energy barriers, which proceeds through the calculation of the adsorption energies at the equilibrium and transition sites. We also discuss finite-size effects and convergence of our results with respect to the lateral dimensions of the slab as well as thickness. Our results are discussed in Sec. III C 3. In Sec. IV, we give a summary.

II. COMPUTATIONAL DETAILS

In order to calculate the energy barriers for adatom diffusion, we construct, for both surfaces of each metal, a five-layer slab such as that depicted in Fig. 1. The supercell, consisting of the slab, the adatom, and a vacuum region (of at least 14 Å), is periodically repeated in space to eliminate boundary effects. In order to maximize the symmetry inside the supercell, we assumed the system to be symmetric with respect to 180° rotations about the x axis lying in the central layer so that, in fact, we have two equivalent surfaces. Each layer of the slab contains four atoms; however, in order to assess finite-size effects, we have examined, in the case of Ag, the dependence of the energy barriers on the size of the layer. Likewise, we have studied for Ag and Ir(111) the dependence on the thickness of the slab; these results are discussed in Sec. III C 2.
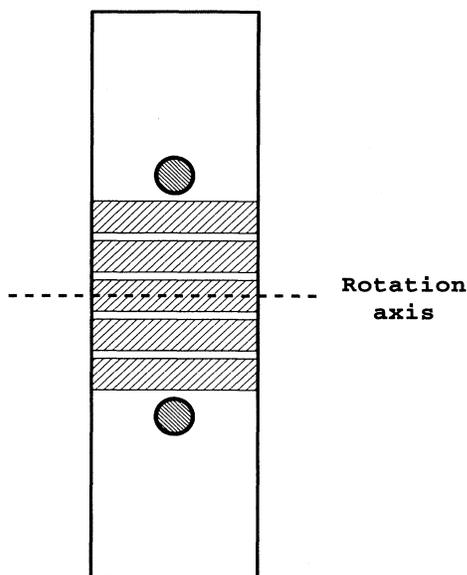
FIG. 1. Schematic representation of the supercell used in the calculations showing the layers, the adatom, and the vacuum region; the central layer contains a rotation axis so that we have, in effect, two equivalent surfaces.

The atoms constituting the slab were initially placed at their exact lattice positions; the appropriate lattice constants were determined from an independent series of calculations for the bulk materials (using one atom per supercell), as discussed in Sec. III A. The geometry of the slab was then "optimized" by relaxing the top layer, i.e., moving it rigidly along the z axis (perpendicular to the surface) until a minimum in energy was found. (Our program has no provisions for calculating the forces.) For this calculation, a "clean" five-layer slab was considered, but using only one atom per layer. Other layers were not moved, since they are generally expected to relax only very little,[32] contributing negligibly to the energy barriers. Our results for the surface relaxation are discussed in Sec. III B.

The calculations were performed as mentioned above, within the framework of density-functional theory[26] in the local-density approximation (LDA).[33] The resulting Kohn-Sham equations were solved using the all-electron FP-LMTO method described in Refs. 15 and 27. Scalar-relativistic corrections were included in all cases. These are essential to reproduce adequately the equilibrium bulk properties of 5d transition metals, while the relativistic LDA calculations are known to underestimate the lattice constant of 4d transition metals by about 2% and to overestimate their bulk moduli by around 25% (Refs. 28 and 34). Considering that these discrepancies are comparable to the error arising from the use of the LDA, and that the reconstruction of 4d metal surfaces has been shown to be rather insensitive to the inclusion of these corrections,[28] we have chosen to include them in all our calculations.

The muffin-tin sphere radius was taken to be 10% less than the contact distance in the bulk configuration. The technique requires nonoverlapping spheres; between the spheres, quantities are extrapolated (using Hankel functions) from their values and slopes at the boundaries of the spheres. Spheres as large as possible are necessary in order to minimize the region where extrapolation is required. However, the spheres must be nonoverlapping, and therefore small enough for the short distances between the adatom and the surface atoms (as well as, to a lesser extent, the surface relaxation) to be properly accounted for. In addition, because of the use of the extrapolation scheme, it is necessary to define "empty spheres" in the vacuum region close to the surface in order to reproduce the exponential decay of the charge density. It was found previously that one layer of empty spheres is sufficient to give a proper description of a clean surface.[27] In our case, because of the presence of an adatom on the surface, two layers of empty spheres were used. For adsorption at the transition state (see Sec. III C 1), a special packing of empty spheres must be used in order to yield, locally, the correct charge density. The optimal arrangement was determined by requiring that the surface energies depend as little as possible on the packing configuration when replacing the adatom by an empty sphere. To minimize numerical errors arising from the packing arrangement, the adsorption energy was in all cases determined by comparing the surface with the adatom with a corresponding clean surface having identical packing of atomic and empty spheres.

The electronic degrees of freedom were treated as follows. For the valence electrons, we used a basis of 27 functions per atom, consisting of s, p, and d functions with kinetic energy $-\kappa^2 = -0.7, -1.0,$ and -2.3 Ry. More explicitly, this basis is 5s, 5p, and 4d for Ag while for Au and Ir it is 6s, 6p, and 5d. In the case of Ir, the spatial extension of the 5p semicore electrons is larger than the size of the spheres and it is necessary to treat them as a full-band state. This is done through a second band-structure calculation ("two-panel" approach), employing a 6s, 5p, and 5d basis. A similar basis has been used successfully in a previous surface study.[27] The core states are recalculated at each iteration in the calculation of the total energy.

All energies were evaluated using the Monkhorst-Pack set of special k points,[35] limited to the irreducible part of the Brillouin zone. The actual number of k points used depends on the size of the Brillouin zone, which itself depends on the size of the system, as well as internal symmetry. (Note that the presence of the adatom reduces the internal symmetry.) In particular, only one point was necessary along the z direction. For the perfect (111) surface with four atoms per layer, the Monkhorst-Pack consists of seven points, and includes the Γ point. For other cases, the number of points was chosen so that the integration over the complete Brillouin zone is performed with a similar k-point density and with comparable accuracy. In the case of (100) surfaces, for consistency with the (111) surfaces, the Monkhorst-Pack points were translated to include the Γ point, while more points were used to compensate for the translation. To ensure numerical stability, finally, the integration was done with a Gaussian broadening of 20 mRy.

III. RESULTS

A. Bulk

We discuss, first, our results for the bulk lattice constants. These are given in Table I; we also present the calculated cohesive energies so as to provide a reference for the adsorption energies. The cohesive energy is simply $E_{coh} = E_{bulk} - E_{atom}$, where E_{bulk} is the energy per atom in the bulk configuration and E_{atom} is the energy of an isolated atom treated using the same scalar-relativistic formalism as for the bulk systems. Low-temperature experimental results are also listed for comparison.

The results for the calculated lattice constants are consistent with the known effects of using the scalar-relativistic procedure: The error (compared to experiment) for the 5d metals is less than 1% while for Ag, a 4d metal, the lattice constant is 1.7% too large. A similar calculation using the same technique, but without relativistic corrections, gives for Ag a lattice constant of 4.09 Å,[29] leading to an accuracy similar to the one we observe here for Au. The cohesive energies, on the other hand, are in rather poor agreement with experiment — systematically overestimated — a well-known deficiency of LDA. In fact, all quantities that involve energy of isolated atoms are poorly described by the LDA. (As we will see below, this problem does not affect the evaluation of the energy barriers.) Again here, for Ag, the agreement is slightly better without relativistic corrections for Ag.[29] The larger error for the cohesive energy of Ir probably arises from the unfilled d shell where spin orientation plays a more important role. (For Rh, its 4d equivalent, a nonrelativistic calculation gives an error of 39% compared to experiment.[29])

B. Clean surfaces

We have calculated, for the various surfaces, the outer-layer relaxation, defined as

$$\Delta d_{12} = \frac{d_{12} - d_{bulk}}{d_{bulk}}, \qquad (3.1)$$

where d_{12} is the distance between the top and the second layer and d_{bulk} is the corresponding interplanar distance in the bulk. At the same time, we have determined the surface energy σ and the work function W. Since the substrate used in these calculations is five layers thick, with one atom per layer, the surface energy per surface atom is given by

$$\sigma = \frac{E_{clean} - 5E_{bulk}}{2}, \qquad (3.2)$$

where E_{clean} is the total energy of the slab supercell. The work function is the difference between the potential energy in the middle of the empty region between the slabs and the Fermi energy.

Results for these quantities are summarized in Table II together with available experimental values. Some of these results have been reported and discussed by other authors[27,28] using similar techniques and will not be examined further here. The results for Au(111) and Ir(111) are (to our knowledge) new; they follow the trends usually observed on fcc metal surfaces, i.e., the surface relaxation and surface energy are smaller than (or equal to) corresponding values on the (100) surface, while it is the opposite for the work function. The surface energies for Ag obtained here are, within 0.01 eV, the same as those obtained without relativistic corrections,[27] which confirms that these corrections have little effect on differences in total energy (and the effect on energy barriers is therefore also small).

TABLE I. Calculated (Calc.) and measured (Expt.) lattice constant a and cohesive energy E_{coh} for the three materials under study.

Material	a (Å)		E_{coh} (eV)	
	Calc.	Expt.[a]	Calc.	Expt.[b]
Ag	4.00	4.07	3.65	2.95
Au	4.06	4.07	4.29	3.81
Ir	3.81	3.83	10.31	6.94

[a]See Ref. 36.
[b]See Ref. 37.

TABLE II. Clean surface properties: top-layer relaxation Δd_{12}, surface energy σ, and work function W. The experimental surface energies are for polycrystalline surfaces. Some of the results have been reported previously using the same technique (Refs. 27 and 28).

Surface	Δd_{12} (%)		σ (J/m^2)		W (eV)	
	Calc.	Expt.	Calc.	Expt.	Calc.	Expt.[g]
Ag(111)	-1.3	< $\lvert 2 \rvert$,[a] 0,[b] -2.5[c]	1.24	1.25[e,f]	5.00	4.74
Ag(100)	-1.9	0 ± 1.5[d]	1.24	1.25[e,f]	4.77	4.64
Au(111)	-0.4		1.32	1.51[e] 1.50[f]	5.80	5.31
Au(100)	-1.0		1.32	1.51,[e] 1.50[f]	5.58	5.47[h]
Ir(111)	-3.0		3.00	3.00[f]	6.15	5.76
Ir(100)	-3.8		3.73	3.00[f]	6.05	5.67

[a]See Ref. 38.
[b]See Ref. 39.
[c]See Ref. 40.
[d]See Ref. 41.
[e]See Ref. 42.
[f]See Ref. 43.
[g]See Ref. 44.
[h]Value for the (1×5) reconstructed surface.

C. Adsorption and diffusion

1. Adsorption energies and energy barriers

We now discuss the energetics of adsorption and diffusion. Using the surfaces relaxed as specified in Sec. III B, it is necessary to first determine the adsorption energy E_{ads} for an adatom at the different sites of interest, namely, the equilibrium site (ES) and the transition site (TS). A schematic view of the potential energy surface seen by an adatom is given in Fig. 2. The equilibrium state, evidently, corresponds to a minimum on the potential energy surface; in order to diffuse to a neighboring site, the adatom must go through a transition state (or bridge position), which corresponds to a saddle point on the potential energy surface. The adsorption energy, at a given site, is

$$E_{ads} = (E_{clean+adatom} - E_{clean} - 2E_{atom})/2, \qquad (3.3)$$

where $E_{clean+adatom}$ is the energy of the supercell slab with the adatom. To minimize the error, as mentioned in Sec. II, we determine the total energies of the two slabs using exactly the same packing of atomic and empty spheres, except that the adatom is replaced by an empty sphere on the clean surface. The optimal position of the adatom, for each site, is determined by displacing it "manually" along the z axis, while constraining the x
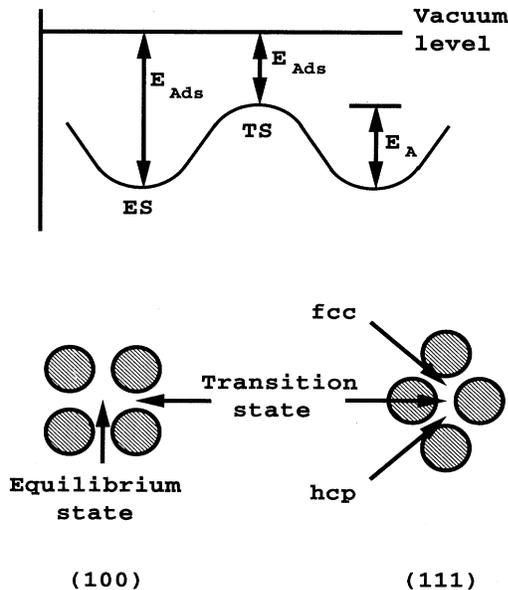

FIG. 2. Top: Schematic representation, in one dimension, of the local potential energy surface seen by a particle diffusing on the surface. We assume here that the particle jumps between two equivalent equilibrium states (ES), via a transition state (TS). The energy barrier for diffusion E_A is simply the difference between adsorption energies at the two sites. Bottom: Top view of the two surfaces locating these sites. Note that the (111) surface of the fcc lattice has two different equilibrium states: the normal site (fcc) and the stacking-fault site (hcp).

and y coordinates, until a minimum of energy is found. As discussed earlier, we neglect here the relaxation of the substrate in the presence of the adatom.

The energy barrier for adatom diffusion is given by

$$E_A = E_{ads}^{ES} - E_{ads}^{TS}. \qquad (3.4)$$

(This difference is independent of E_{atom} and therefore not affected by errors in this quantity, as mentioned above.) The equilibrium and transition sites for the two kinds of surfaces studied here are identified in Fig. 2. The (100) surface is a simple square lattice, and all equilibrium states equivalent. The (111) surface, on the other hand, has hexagonal symmetry, with two nonequivalent equilibrium sites: the normal (or fcc) site, and the stacking-fault (or hcp) site. (The hcp site has an atom directly under it in the second layer, while the fcc site has one, rather, in the third layer.) In this case we take, for E_{ads}^{ES} in Eq. (3.4), the value with the largest adsorption energy (i.e., the site which sits deepest).

The results for the equilibrium-site adsorption energies are given in Table III. The estimated error on these numbers is about 0.01 eV, as deduced from the convergence of the total energy and the resolution of the z grid. The adatom is bonded more strongly on the (100) surface than on the (111), owing to the fact that coordination is larger on the former than on the latter (four versus three). The calculated differences in energy between the hcp and fcc sites on the (111) surfaces are very small (less than 0.02 eV, i.e., not really significant), and comparable to measured values [0.022 eV in favor of the fcc site for Ir/Ir(111) (Ref. 13)]. In subsequent calculations, we assume the two equilibrium sites on the (111) surfaces to be equivalent, and therefore take the transition state to be exactly midway between them, although E_A is taken as the energy to escape the most favorable site. Before discussing the calculated activation energies, we examine the convergence of our results with respect to possible finite-size effects.

2. Finite-size effects

The calculations reported here are computationally intensive, and it is only possible to deal with small systems. It is essential, therefore, to estimate the importance of finite-size contributions to the calculated properties. We have carried out a series of tests on the (111) and (100) surfaces of Ag; this material is more amenable to finite-size tests because it contains fewer electrons than Au and Ir. In what follows, we discuss the variations of the

TABLE III. Adsorption energies E_{ads}, in eV, for an adatom on the (100) and (111) surfaces using a five-layer thick, four-atom-per-layer substrate.

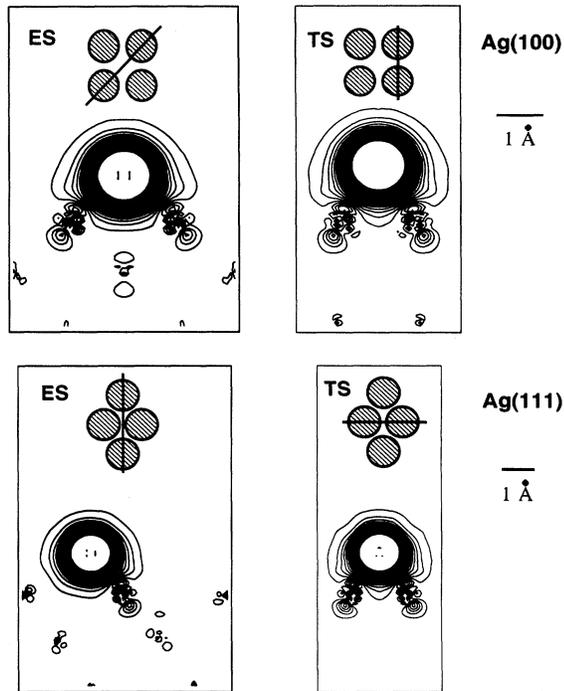| Material	(100)	(111)-fcc	(111)-hcp
Ag	2.99	2.82	2.84
Au	3.71	3.33	3.31
Ir	9.07	7.68	7.69

FIG. 3. Difference in charge density due to the presence of the adatom on the Ag (100) (top) and (111) (bottom) surfaces for a five-layer slab, on the planes as defined in the insets (left, ES; right, TS).

TABLE IV. Variation of the energy barrier E_A, in eV, with substrate thickness and lateral dimensions, compared to a five-layer thick, four-atom-per-layer substrate.

Surface	7 vs 5 layers	6 vs 4 atom/layer	9 vs 4 atom/layer
Ag(111)	0.01		0.00
Ag(100)	-0.01	-0.07	-0.07
Ir(111)	0.01		

results presented in Sec. III C 1 as a function of both substrate thickness and lateral dimensions (i.e., number of atoms per layer).

The importance of the thickness of the substrate can be qualitatively assessed by examining changes in electron density resulting from the presence of the adatom, $\rho_{clean+adatom} - \rho_{clean}$. In Fig. 3, we show this quantity for our two Ag surfaces, for the planes indicated by the straight lines in the insets. It is clear, from Fig. 3, that only the transition state of the (111) surface is well described by a five-layer substrate, since in this case $\rho_{clean+adatom} - \rho_{clean}$ vanishes in the middle of the substrate. In order to get a quantitative estimate of the observed differences, we have repeated the calculation of

the adsorption energies of both Ag surfaces using, this time, a seven-layer substrate. The results are reported in Table IV. We find, which is reassuring, that the energy barrier E_A is rather insensitive to the thickness of the substrate, the difference being within the error bar of the calculations; a five-layer substrate, therefore, is sufficient to yield converged results. We have, in fact, verified this on the Ir(111) surface, as reported in Table IV. It should be noted, however, that while the energy difference E_A, Eq. (3.4), remains constant, the adsorption energies for the (100) surface vary quite substantially, by about 0.1 eV upon changing the thickness of the substrate from five to seven layers.

We have also examined the variations of E_A with the lateral system size using a five-layer slab with nine atoms per layer. This size is such that the symmetry of the (111) surface is preserved; for the (100) surface, it is also possible to consider the case of six atoms per layer without breaking the local symmetry. The results are reported in Table IV. We find the (111) surface of Ag to remain essentially unchanged upon going to a larger system, while the (100) surface is affected significantly. In the latter case, it appears that a six-atom-per-layer slab is sufficient to yield converged results. The variations observed on the (100) surface arise mainly from changes in the adsorption energy at the transition state: within error, the adsorption energy at the equilibrium state remains constant with size.

In summary, to obtain converged values for the energy barriers on these surfaces, it is sufficient to use a five-layer slab with four atoms per layer, except for the transition state on the (100) surface where at least six atoms per layer are needed. The size-corrected values of E_A, obtained by a new set of calculations fulfilling the previous conditions for convergence of the barrier on the (100) surface, are listed in Table V where we also give, for compar-

TABLE V. Calculated and measured energy barriers E_A, in eV. The calculated values are obtained using the cell size discussed in Sec. III C 2.

Surface	Present work	EAM, EMT or RGL	Expt.
Ag(111)	0.14±0.02	0.06,[a] 0.12,[b] 0.064[c]	0.15±0.1[b]
Ag(100)	0.50±0.03	0.47,[a] 0.365[c]	
Au(111)	0.22±0.03	0.02,[a] 0.102[c]	
Au(100)	0.62±0.04	0.64,[a] 0.490[c]	
Ir(111)	0.24±0.03	0.11,[d] 0.19[d]	0.22±0.03,[e] 0.267±0.003[f]
Ir(100)	1.39±0.04	1.58,[d] 1.57[d]	

[a]See Ref. 16.
[b]See Ref. 9.
[c]See Ref. 46.

[d]See Ref. 45.
[e]See Ref. 10.
[f]See Ref. 13.

ison, the experimental values (where available), as well as the values obtained using semiempirical models — either EAM,[16,45] the effective-medium theory (EMT),[9,46] or the glue model of Rosato, Guillope, and Legrand (RGL).[45]

3. Discussion

The results presented in Table V lead to several observations. First, the energy barriers are found to be lower on the (111) than on the (100) surface, as expected, since the former is more closed packed. Considering the low values obtained on the (111) surface, diffusion should proceed rather easily on this surface, even at low temperatures.

Second, the agreement with the experimental results is excellent, within the combined error bar of calculation and experiment, i.e., no more than 0.03 eV. This confirms that the relaxation of the substrate around the adatom, which we ignore here, has negligible effect on the energy barriers for the (111) surfaces. This is in line with corresponding calculations for Pt/Pt(111) (Ref. 30) and Ag/Pt(111),[31] which demonstrate that energy barriers change only very slightly when nearest-neighbor relaxation is taken into account [from 0.41 to 0.38, i.e., −0.03 eV for Pt/Pt(111), and from 0.21 to 0.20, i.e., −0.01 eV for Ag/Pt(111)]. Experimental values for the energy barriers on the other surfaces are not (to our knowledge) available, but it would be of considerable interest that our theoretical predictions be confirmed.

Upon comparing the FP-LMTO results with the values from semiempirical models, we find that the latter seriously underestimate the barriers on the (111) surfaces. (One exception is the EMT value for Ag(111),[9] which is in good accord with experiment.) On the other hand, the value for Ir(100) is largely overestimated. In fact, the semiempirical models seem to reproduce the energy barriers to within about 0.2 eV; such errors are dramatic when examining the temperature behavior of the diffusion coefficient. Nevertheless, in some cases, Ag(100), (111), and Au(100), the energy barriers from the semiempirical models are within the error bar of the first-principles calculations.

It is instructive to compare the energy barriers of the various surfaces with the corresponding bulk melting temperatures. As mentioned earlier, we have demonstrated in a previous EAM study[16] that diffusion becomes non-Arrhenius at temperatures corresponding to about half of the static energy barrier, owing to the existence at "high" temperatures of correlations between jumps. From the values given in Table V, we conclude that the random-walk model is appropriate for the Au(111) surface, since the barrier on this surface, 0.24 eV, is somewhat larger than the melting-point energy (of the bulk material), 0.115 eV, while this is not the case for Ag(111) and Ir(111), for which the barrier and the melting temperatures are comparable (0.14 versus 0.106 eV for Ag, and 0.24 versus 0.234 eV for Ir). Thus, at sufficiently high temperatures, non-Arrhenius diffusion must be the rule on Ag(111) and Ir(111). We note that a recent first-principles calculation[47] for Al/Al(111) gave a barrier for diffusion of 0.04 eV, sizeably smaller than

the melting point of the material, 0.080 eV. This system, therefore, should definitely exhibit non-Arrhenius behavior, i.e., correlated jumps, over a wide range of temperatures. It would be of interest to carry out an experimental verification of this prediction.

Likewise, diffusion is very well approximated by a random walk on the (100) surfaces, which have barriers much larger than the melting-point energies. We note, however, that the energy barrier for Ir is so large that diffusion can only take place at high temperatures. This is consistent with the experimental observation — inferred from a detailed mapping of the position of the adatom — that diffusion on this surface, at low temperature, proceeds via an exchange mechanism.[8]

We note, as a final point, that calculations of the energy barriers for Pt/Pt(111) and Ag/Pt(111) using the scattering-theory method were reported recently.[30,31] The barriers were found to be larger than the measured values by, respectively, 0.13 and 0.04 eV. While the latter compares well with experiment, the discrepancy for the former, is significantly higher. The large error was attributed to the larger adsorption energy of the Pt adatom compared to the Ag adatom.[31] While this is a possibility, our calculations indicate that this might not be the proper explanation. [Ir/Ir(111) has a higher adsorption energy than Pt/Pt(111), and yet is well accounted for by our approach.] It is also indicated in Ref. 31 that the relaxation of the second and subsequent neighbors, which was ignored, could have an effect on the barrier. We are currently examining the case of Pt/Pt(111) in order to resolve this point.

IV. SUMMARY

We have used the FP-LMTO method to calculate the energy barriers for adatom homodiffusion on the (111) and (100) surfaces of Ag, Au, and Ir. Our results agree very well with the measured energy barriers (when available), i.e., to within 0.03 eV, thereby confirming the adequacy of the theoretical method. On the (111) surfaces, we find that the barriers for Ag and Ir have values that are close to those corresponding to the melting point of the bulk materials and conclude, therefore, that correlated jumps should be present at high temperatures on these surfaces. For Au(111), on the other hand, the barrier is about twice as large as the melting temperature; the random-walk model should provide an accurate description of the diffusion process, just as on the (100) surfaces, where the barriers are much larger. Semiempirical models are found to reproduce the first-principles energy barriers within 0.2 eV, which, in some cases, translates into errors as large as 90%. It would be of considerable interest that experimental measurement of our predicted energy barriers be carried out.

ACKNOWLEDGMENTS

* Electronic address: boisver@physcn.umontreal.ca

† Author to whom correspondence should be addressed; electronic address: lewis@physcn.umontreal.ca

[1] See, for instance, *Evolution of Surface and Thin Film Microstructure*, edited by H.A. Atwater, E. Chason, M.H. Grabow, and M.G. Lagally, MRS Symposia Proceedings No. 280 (Materials Research Society, Pittsburgh, 1993).

[2] M. Zinke-Allmang, L.C. Feldman, and M.H. Grabow, Surf. Sci. Rep. **16**, 377 (1992).

[3] J.A. Venables, Philos. Mag. **27**, 697 (1973).

[4] R. Gomer, Rep. Prog. Phys. **53**, 917 (1990).

[5] T.T. Tsong, Rep. Prog. Phys. **51**, 759 (1988).

[6] D.W. Bassett and P.R. Webber, Surf. Sci. **70**, 520 (1978).

[7] R.T. Tung and W.R. Graham, Surf. Sci. **97**, 73 (1980).

[8] C. Chen and T.T. Tsong, Phys. Rev. Lett. **64**, 3147 (1990).

[9] G.W. Jones, J.M. Marcano, J.K. Nørskov, and J.A. Venables, Phys. Rev. Lett. **65**, 3317 (1990).

[10] C. Chen and T.T. Tsong, Phys. Rev. B **41**, 12403 (1990).

[11] G.L. Kellogg, Surf. Sci. **246**, 31 (1991).

[12] G.L. Kellogg, A.F. Wright, and M.S. Daw, J. Vac. Sci. Technol. A **9**, 1757 (1991).

[13] S.C. Wang and G. Ehrlich, Phys. Rev. Lett. **68**, 1160 (1992).

[14] G.L. Kellogg, Surf. Sci. **266**, 18 (1992).

[15] M. Methfessel, Phys. Rev. B **38**, 1537 (1988); M. Methfessel, C.O. Rodriguez, and O.K. Andersen, *ibid.* **40**, 2009 (1989).

[16] G. Boisvert and L.J. Lewis, in *Mechanisms of Thin-Film Evolution*, edited by S.M. Yalisove, C.V. Thomson, and D.J. Eaglesham, MRS Symposia Proceedings No. 317 (Materials Research Society, Pittsburgh, 1994), p. 71; G. Boisvert and L.J. Lewis (unpublished).

[17] S.M. Foiles, M.I. Baskes, and M.S. Daw, Phys. Rev. B **33**, 7983 (1986).

[18] G. Boisvert, L.J. Lewis, and A. Yelon, Phys. Rev. Lett. **75**, 469 (1995).

[19] A.R. Sandy, S.G.J. Mochrie, D.M. Zehner, K.G. Huang, and D. Gibbs, Phys. Rev. B **43**, 4667 (1991).

[20] G. Boisvert and L.J. Lewis, in *Physics Computing 94*, edited by by R. Gruber and M. Tomassini (European Physical Society, Geneva, 1994), p. 29.

[21] D.W. Bassett and P.R. Webber, Surf. Sci. **70**, 520 (1978).

[22] K. Heinz, G. Schmidt, L. Hammer, and K. Müller, Phys. Rev. B **32**, 6214 (1985).

[23] B.M. Ocko, D. Gibbs, K.G. Huang, D.M. Zehner, and S.G.J. Mochrie, Phys. Rev. B **44**, 6429 (1991).

[24] P.J. Feibelman, Phys. Rev. Lett. **65**, 729 (1990).

[25] R. Stumpf and M. Scheffler, Surf. Sci. **307-309**, 501 (1994).

[26] W. Kohn and L.J. Sham, Phys. Rev. **140**, A1133 (1965).

[27] M. Methfessel, D. Hennig, and M. Scheffler, Phys. Rev. B **46**, 4816 (1992).

[28] V. Fiorentini, M. Methfessel, and M. Scheffler, Phys. Rev. Lett. **71**, 1051 (1993).

[29] H.M. Polatoglou, M. Methfessel, and M. Scheffler, Phys. Rev. B **48**, 1877 (1993).

[30] P.J. Feibelman, J.S. Nelson, and G.L. Kellogg, Phys. Rev. B **49**, 10548 (1994).

[31] P.J. Feibelman, Surf. Sci. Lett. **313**, L801 (1994).

[32] A.M. Rodríguez, G. Bozzolo, and J. Ferrante, Surf. Sci. **289**, 100 (1993).

[33] D.M. Ceperley and B.J. Alder, Phys. Rev. Lett. **45**, 566 (1980); J. Perdew and A. Zunger, Phys. Rev. B **23**, 5048 (1981).

[34] C. Elsässer, N. Takeuchi, K.M. Ho, C.T. Chan, P. Braun, and M. Fähnle, J. Phys. Condens. Matter **2**, 4371 (1990).

[35] H.J. Monkhorst and J.D. Pack, Phys. Rev. B **13**, 5188 (1976); J.D. Pack and H.J. Monkhorst, *ibid.* **16**, 1748 (1977).

[36] Y.S. Touloukian, R.K. Kirby, R.E. Taylor, and P.D. Desai, *Thermophysical Properties of Matter*, Thermal Expansion—Metallic Elements and Alloys Vol. 12 (Plenum, New York, 1975).

[37] C. Kittel, *Introduction to Solid State Physics*, 6th ed. (Wiley, New York, 1986).

[38] R.J. Culbertson, L.C. Feldman, P.J. Silverman, and H. Böhm, Phys. Rev. Lett. **47**, 657 (1981).

[39] F. Soria, J.L. Sacedon, P.M. Echenique, and D. Titterington, Surf. Sci. **68**, 448 (1977).

[40] P. Statiris, H.C. Lu, and T. Gustafsson, Phys. Rev. Lett. **72**, 3574 (1994).

[41] H. Li, J. Quinn, Y.S. Li, D. Tian, F. Jona, and P.M. Marcus, Phys. Rev. B **43**, 7305 (1991).

[42] W.R. Tyson and W.A. Miller, Surf. Sci. **62**, 267 (1977).

[43] F.R. De Boer, R. Boom, W.C.M. Mattens, A.R. Miedema, and A.K. Niessen, *Cohesion in Metals* (North-Holland, Amsterdam, 1988).

[44] *Handbook of Chemistry and Physics*, 70th ed., edited by R.C. Weast (CRC Press, Boca Raton, FL, 1989).

[45] K.D. Shiang, C.M. Wei, and T.T. Tsong, Surf. Sci. **301**, 136 (1994); for details of the RGL model, see V. Rosato, M. Guillope, and B. Legrand, Philos. Mag. A **59**, 321 (1989).

[46] P. Stoltze, J. Phys. Condens. Matter **6**, 9495 (1994).

[47] R. Stumpf and M. Scheffler, Phys. Rev. Lett. **72**, 254 (1994).